Chinese Chemical Letters 37 (2026) 111539

Contents lists available at ScienceDirect

Chinese Chemical Letters

journal homepage: www.elsevier.com/locate/cclet

Icaritin-incorporated dual-sensitizing hydrogel for osteosarcoma doxorubicin treatment and bone regeneration

Qing-Ri Jin[a,1], Tian-Jiao Zhou[b,1], Ya-Ting Yao[b,1], Hai-Qing Yu[b], Hao-Bin Che[b], Meng-Meng Zhang[b], Chun-Hui Cui[b], Yi Wang[b], Cheng-Jun Li[c,*], Lei Xing[b,*], Hu-Lin Jiang[b,d,e,*]

[a] School of Pharmacy, Hangzhou Medical College, Hangzhou 311399, China
[b] State Key Laboratory of Natural Medicines, China Pharmaceutical University, Nanjing 210009, China
[c] Department of Orthopedics, Jinling Hospital, School of Medicine, Nanjing University, Nanjing 210002, China
[d] College of Pharmacy, Yanbian University, Yanji 133002, China
[e] Department of Precision Medicine, School of Medicine, Sungkyunkwan University, Suwon 16419, South Korea

ARTICLE INFO

Article history:
Received 11 February 2025
Revised 1 July 2025
Accepted 2 July 2025
Available online 3 July 2025

Keywords:
Osteosarcoma
Thermosensitive hydrogel
Doxorubicin hydrochloride
Icaritin
Pluronics

ABSTRACT

Osteosarcoma (OS) is the most common primary bone malignancy. However, treatment remains challenging due to multidrug resistance, toxic side effects from high-dose and frequent chemotherapy, and surgery-induced bone defects. Herein, we report a double-sensitizing chemotherapeutic hydrogel for efficient OS treatment and bone regeneration, which is constructed by loading doxorubicin hydrochloride (DOX) and icaritin (ICT) into Pluronic F127 (F127) and Pluronic F68 (F68) hydrogel matrix (DOX/ICT-gel). Both ICT and Pluronics can sensitize cancer cells to DOX treatment and enhance intracellular DOX accumulation, thereby boosting the cytotoxic activity of DOX. The addition of ICT can not only downregulate the required dose of DOX and reduce the toxic side effects of DOX, but also induce osteoblast differentiation, contributing to bone regeneration. In the *in-situ* anti-OS study, the DOX/ICT-gel was shown to stay locally for 7 days, and effectively inhibits OS tumor growth and metastasis, providing robust anticancer efficacy with low toxicity from a single injection for long-lasting treatment. This research provides a novel dual-sensitive DOX strategy for localized OS therapy, potentially advancing the clinical management of this challenging disease.

© 2026 Published by Elsevier B.V. on behalf of Chinese Chemical Society and Institute of Materia Medica, Chinese Academy of Medical Sciences.

Osteosarcoma (OS) is the most common primary malignant bone tumor in children and adolescents [1–3], and remains the second leading cause of cancer-related death in this age group [4]. Due to its aggressive local invasion and high recurrence rate after surgery, children and adolescents with OS may suffer lifelong disability or even death, placing a heavy burden on their families and society. Despite advances in treatment, the survival rate for OS patients has not improved significantly over the past four decades [5]. Current treatment typically involves preoperative (neoadjuvant) chemotherapy, surgical resection, and postoperative (adjuvant) chemotherapy [6,7]. Among them, doxorubicin hydrochloride (DOX) is the most commonly used chemotherapeutic agent for OS [8], however, its long-term use is associated with drug resistance and severe toxic side effects, particularly damage to the heart and kidneys, and inhibit bone marrow regeneration [9–13]. Given these challenges, we hypothesize that a drug combination strategy could enhance the efficacy of DOX in OS treatment while reducing both its toxicity and the development of multidrug resistance. Such a combination might target the underlying mechanisms of resistance or protect healthy tissues, offering a promising approach to improving survival outcomes and minimizing adverse effects in OS patients.

Chinese herbal medicine, with a rich history spanning over 5000 years, has demonstrated significant therapeutic potential in treating a variety of diseases. As research in natural medicine chemistry has advanced, the active compounds in traditional Chinese medicine have garnered attention for their promising roles in cancer therapy [6,14–16]. Combining traditional Chinese medicine with conventional chemotherapy has shown advantages, such as enhancing chemotherapy drug sensitivity and reducing drug resistance in tumors [17–19]. Among the vast array of Chinese herbs,

* Corresponding authors.
E-mail addresses: 48933897@qq.com (C.-J. Li), xinglei6xl@163.com (L. Xing), jianghulin3@163.com (H.-L. Jiang).
[1] These authors contributed equally to this work.

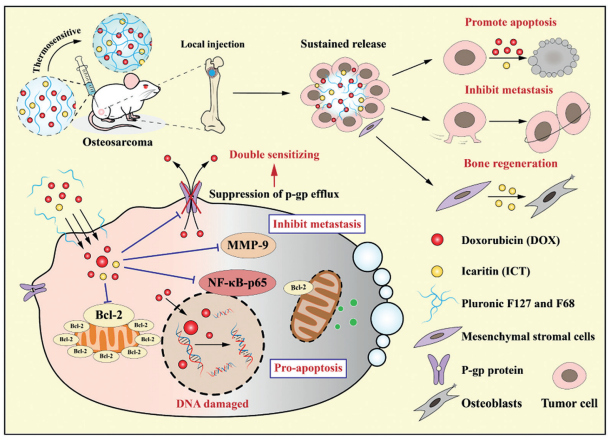
https://doi.org/10.1016/j.cclet.2025.111539
1001-8417/© 2026 Published by Elsevier B.V. on behalf of Chinese Chemical Society and Institute of Materia Medica, Chinese Academy of Medical Sciences.

icaritin (ICT), a prenylflavonoid derived from the herb *Epimedium*, stands out. ICT was recognized by the Chinese Society of Clinical Oncology (CSCO) guidelines as a systemic treatment for advanced hepatocellular carcinoma (HCC), marking it as the world's first-in-class small molecule immunomodulator with independent intellectual property rights in China [20,21]. ICT has demonstrated efficacy in remodeling the immunosuppressive tumor microenvironment and enhancing the anticancer effects of chemotherapy, particularly in combination with DOX in HCC treatment [22]. In addition to its anticancer properties, *Epimedium* is traditionally used in Chinese medicine to strengthen bones and tendons, and ICT has been shown to promote bone regeneration, making it a promising candidate for enhancing anti-OS efficacy and bone regeneration [23]. Given these properties, we hypothesize that combining ICT with DOX could offer a novel and effective treatment strategy for OS, leveraging both the anticancer effects and bone-regenerative potential of ICT.

Traditional systemic drug delivery often faces challenges in oncology, including low efficacy and high organ toxicity, as chemotherapy drugs are quickly metabolized, making it difficult to reach targeted tumor cells [24]. In recent years, *in-situ* gel systems have gained attention for their ability to provide continuous drug release, reduce systemic toxicity, and decrease the frequency of administration [25–30]. Among these, thermo-sensitive hydrogels are particularly promising [31]. Pluronics F68 and F127, two U.S. Food and Drug Administration (FDA)-approved classes of Pluronics, are widely used as materials for *in vivo* applications [32]. When the concentration of F127 reaches 18%, the solution forms a gel upon reaching its phase-transition temperature, making it a suitable thermosensitive hydrogel [33–35]. These Pluronic block copolymers consist of triblock polyethylene oxide–propylene oxide–polyethylene oxide (PEO–PPO–PEO) structures and self-assemble into micelles, with a hydrophobic PPO core and a hydrophilic PEO shell, which can enhance the solubility of lipophilic drugs by encapsulating them in the core. Importantly, Pluronic block copolymers have been shown to interact with multidrug-resistant (MDR) cancer cells, increasing their sensitivity to various anticancer agents, especially anthracyclines like DOX [36]. This interaction makes F127 an ideal candidate to partner with DOX, enhancing its efficacy while potentially overcoming drug resistance.

In this study, we developed an F68/F127 temperature-sensitive injectable hydrogel loaded with DOX and ICT for the treatment of OS, named as DOX/ICT-gel. As illustrated in Scheme 1, both DOX and ICT are fully dissolved in F68/F127 solution. Upon injection into tumor tissues, the solution transforms into a hydrogel at body temperature and then continuously releases DOX and ICT into tumor cells. DOX induces tumor cell death by entering the cell nucleus and preventing DNA replication [37]. With the assistance of ICT and F127, the nuclear accumulation of DOX is enhanced with DOX/ICT-gel treatment, leading to apoptosis *via* the inhibition of nuclear factor kappa B (NF-κB) and B-cell lymphoma (Bcl)-2 signaling pathways [38]. In addition, DOX/ICT-gel reduces tumor metastasis by downregulating matrix metalloproteinase (MMP)-9 expression as evidenced by significant inhibition of tumor growth and metastasis in both *in vitro* and *in vivo* models. Additionally, ICT contributes to bone regeneration, offering significant potential for enhancing OS treatment outcomes and promoting healing of affected bone tissue.

First, F127/F68 hydrogel solutions were prepared using a cold method, and the optimal concentrations and ratios of F127 and F68 were determined by evaluating the gelation temperature (Table S1 in Supporting information). For ease of injection, the hydrogel is preferably kept in a sol state at room temperature and converted into a gel after being injected into the tumor. As shown in Figs. S1 and S2 (Supporting information), a ratio of 28% F127 and 18% F68 was selected after optimization. This high concentration of F127 extended the release time of the hydrogel. For the preparation of DOX/ICT-gel, DOX was dissolved in a NaCl solution, followed by the addition of F127 and F68 using the cold method. Next, ICT DMSO was added and stirred vigorously at ice bath. ICT-gel and DOX-gel were prepared using the same method. The sol-gel transformation was tested by the tube inversion method, and the phase transition temperature of the gel solution containing 28% F127 and 18% F68 is 29 °C. As shown in Fig. 1a, the hydrogel solution is soluble at 4 °C and transitions to a gel at 37 °C. And the DOX/ICT-gel immediately forms a gel upon injection into a 37 °C phosphate buffered saline (PBS) solution using a syringe with a 0.45 mm inner diameter, indicating that it forms a gel *in vivo* as well (Fig. 1b). The gelation time is summarized in Table S2 (Supporting information), showing that adding DOX and ICT could shorten the gelation time. The three-dimensional porous structure of the DOX/ICT-gel was observed using scanning electron microscopy (SEM) after gelation (Fig. 1c), indicating a high surface area and interconnected network and facilitating sustained drug release and enhanced cellular infiltration for improved therapeutic efficacy in osteosarcoma treatment.



Scheme 1. The flowable liquid state (sol) to semi-solid hydrogel (gel) transformation of DOX/ICT-gel and its anticancer mechanism during OS treatment. The *in-situ* injection of DOX/ICT-gel enables the slow release of DOX and ICT. ICT and Pluronic can augment intracellular accumulation of DOX. The synergistic effect of ICT and DOX induces apoptosis by inhibiting the NF-κB and Bcl-2 signaling pathways, while simultaneously promoting osteoblast differentiation, thereby contributing to bone regeneration. Additionally, the DOX/ICT-gel effectively inhibits OS metastasis by downregulating the expression of MMP-9.

Next, the rheological properties of the hydrogel were evaluated. As shown in Fig. 1d and Fig. S3 (Supporting information), the hydrogel undergoes a gel transition at room temperature when the F127:F68 ratio is 28%:18%, which is important for maintaining gel stability at body temperature. The incorporation of DOX and ICT did not significantly affect the rheological properties or gelation temperature, indicating that both drugs are compatible with the hydrogel matrix and do not disrupt its structure. To study hydrogel degradation and drug release, DOX/ICT-gel was incubated in PBS with different pH values at 37 °C, and the PBS solution was replaced every 8 h. The weight of the remaining hydrogel was measured at each PBS change and the drug release was monitored. As shown in Figs. 1e–g, the DOX/ICT-gel was completely eroded after 96 h of incubation, and the drug was also completely released at this time, indicating that the drug release was mainly affected by the dissolution of the hydrogel. Additionally, the hydrogel showed higher weight loss and drug release at acidic pH (pH 6.5) compared to neutral pH (pH 7.4), indicating that the hydrogel degrades faster in acidic conditions, enhancing drug release in tumor. Finally, the hemolysis test was conducted to assess the blood compatibility of

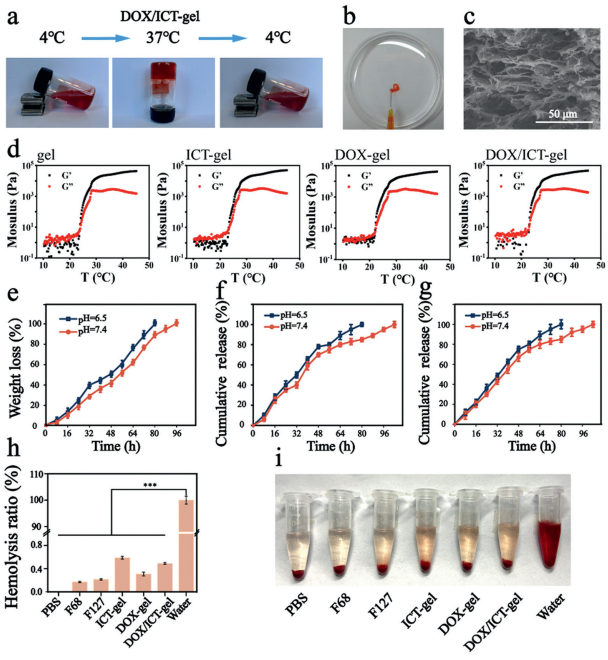


Fig. 1. Characterization of DOX/ICT-gel. (a) Phase transition of DOX/ICT-gel at 4 and 37 °C. (b) Injectability of DOX/ICT-gel through a syringe with an internal diameter of 0.45 mm into 37 °C PBS solution. (c) SEM image of DOX/ICT-gel (scale bar: 50 μm). (d) Rheological analysis of blank gel, ICT-gel, DOX-gel, and DOX/ICT-gel. (e) Weight loss of DOX/ICT-gel in PBS solution at different pH values (7.4 and 6.5). Cumulative release of (f) DOX and (g) ICT from DOX/ICT-gel in PBS solution at different pH values. (h) Hemolysis ratio and (i) images of erythrocyte hemolysis after incubation with different groups at 37 °C for 1 h. Data are presented as mean ± standard deviation (SD) ($n = 3$). $^{***}P < 0.001$.

the hydrogel [39]. PBS, F68, F127, ICT-gel, DOX-gel, and DOX/ICT-gel were incubated with red blood cells for 1 h, and the hemolysis of different groups was determined by detecting the absorbance in the supernatant. As shown in Figs. 1h and i, the hemolysis rate of the hydrogel group was significantly lower than that of the pure water group (<4 %), indicating that DOX/ICT-gel has good blood compatibility and is expected to be injected locally at the tumor site to avoid hemolysis and inflammatory response.

The anticancer efficacy of the DOX/ICT-gel was evaluated in the K7M2 mouse OS cell line. To determine the optimal ratio of DOX and ICT, we first conducted a combination index (CI) assay. As shown in Fig. 2a and Table S3 (Supporting information), the best synergistic effect of free DOX to free ICT was achieved at a 5:1 ratio, which was used for subsequent experiments. Next, the toxicity of different hydrogel formulations was assessed using the methylthiazolyldiphenyl-tetrazolium bromide (MTT) assay. In order to more accurately compare the efficacy of free DOX and different hydrogel formulations and evaluate the sensitizing effect of F68/F127 and ICT on the anticancer efficacy of DOX, the sol formulations were directly dispersed into the culture medium and incubated with cells in the cell-level study. Fig. 2b and Fig. S4 (Supporting information) show that neither F68 nor F127 exhibited toxicity to K7M2 cells. Next, the toxicity of free ICT, ICT-sol, free DOX, DOX-sol and DOX/ICT-sol was tested. The experimental results are shown in Figs. 2c and d. Compared with free ICT and DOX, the sol formulation can significantly increase the toxic effect of the drug on K7M2. ICT-sol shows mild toxicity starting at a concentration of 5 μmol/L, while DOX-sol demonstrates inhibitory effects at a concentration of 1 μmol/L. As shown in Fig. 2e, DOX-sol showed a significant inhibitory effect on K7M2 cells at a concentration greater than 2 μmol/L, but the DOX/ICT-sol group significantly enhanced the anticancer effect of DOX at a lower concentration, indicating that ICT may enhance DOX efficacy through a synergistic mechanism rather than by its cytotoxicity. The half maximal inhibitory concentration (IC_{50}) of DOX-sol was 3.691 μmol/L, and the IC_{50} of DOX/ICT-sol was 1.581 μmol/L, indicating that the addition of ICT significantly increased the toxic effects of the DOX/ICT-sol group. As shown in Fig. 2f, ICT-sol alone did not induce significant apoptosis in K7M2 cells. DOX-sol treatment induced early apoptosis, while DOX/ICT-sol combined treatment induced more significant apoptosis and mostly late-onset apoptosis, indicating that the combined action of DOX and ICT can enhance the cytotoxicity to K7M2 cells. The cytotoxic effects of DOX/ICT-sol were further confirmed by live/dead staining. In Fig. 2g and Fig. S5 (Supporting information), red fluorescence (indicating dead cells) was significantly stronger in the DOX/ICT-sol group compared to the F68, F127, ICT-sol, and DOX-sol groups, while green fluorescence (indicating live cells) was weaker. This suggests that DOX/ICT-sol had a stronger killing effect on K7M2 cells than ICT-sol or DOX-sol alone.

The biocompatibility of DOX/ICT-sol and its toxicity toward normal cells were also assessed. MTT assays on L02 (human hepatocyte) cells revealed that F68, F127, ICT-sol, DOX-sol, and DOX/ICT-sol did not significantly affect cell viability after 24 h of incubation (Figs. 2h–j and Fig. S6 in Supporting information). Additionally, DOX/ICT-sol did not exhibit significant toxicity toward mesenchymal stem cells (MSCs) (Fig. 2k), which can differentiate into osteoblasts and promote bone regeneration. This selective cytotoxicity may be attributed to the higher proliferative rate of K7M2 cells, which renders them more susceptible to DNA synthesis inhibitors such as DOX. Therefore, DOX-sol and DOX/ICT-sol have stronger killing effects on K7M2 cells with strong proliferation ability but have no obvious killing effect on normal cells L02 cells at the same concentration, and can even increase the cell viability of MSCs [40].

The high mortality rate of OS is primarily attributed to the metastasis of *in-situ* cancerous tissues, therefore, to evaluate the effect of DOX/ICT-sol on the migration and invasion of K7M2 cells, we conducted wound healing assays and Transwell invasion assays [41]. As shown in Figs. 3a and b, the migration rate of cells in the control, F68, and F127 groups was approximately 45 %–50 % after 24 h incubation. ICT-sol treatment showed a slight inhibitory effect, while DOX-sol significantly reduced the migration of K7M2 cells. Notably, the DOX/ICT-sol group exhibited the most pronounced inhibition of migration compared to the other treatment groups ($P < 0.001$). In the Transwell invasion assay, K7M2 cell suspensions were added to Transwell chambers, and the cells were treated with F68, F127, ICT-sol, DOX-sol, or DOX/ICT-sol diluted in DMEM containing 5 % fetal bovine serum (FBS). After 24 h of incubation, the cells that had penetrated the membrane were stained with crystal violet and observed under a microscope. The control group showed a high level of invasion, with most cells penetrating the membrane. In contrast, the number of invading cells decreased following treatment with DOX-sol and ICT-sol, with the DOX/ICT-sol group showing the least number of membrane-penetrating cells (Figs. 3c and d). These results collectively indicate that DOX/ICT-sol has the most effective inhibitory effect on the migration and invasion of K7M2 cells, suggesting its potential to reduce OS metastasis.

To further investigate the mechanism underlying the inhibitory effects of DOX/ICT-sol on the proliferation and metastasis of K7M2 cells, we examined the expression levels of key proteins involved in drug resistance, apoptosis, and metastasis: P-glycoprotein (P-gp), NF-κB-p65, Bcl-2, and MMP-9. P-gp is an ATP-dependent efflux pump that reduces intracellular drug concentrations by expelling therapeutic agents from the cell, contributing significantly to multidrug resistance in tumors. NF-κB, a transcription factor, is essential for regulating tumor growth, survival, invasion, and chemoresistance in OS [42,43]. Bcl-2, an anti-apoptotic protein, is commonly overexpressed in OS and is associated with chemoresistance and poor prognosis [44–46]. Additionally, MMP-9, a metallo-

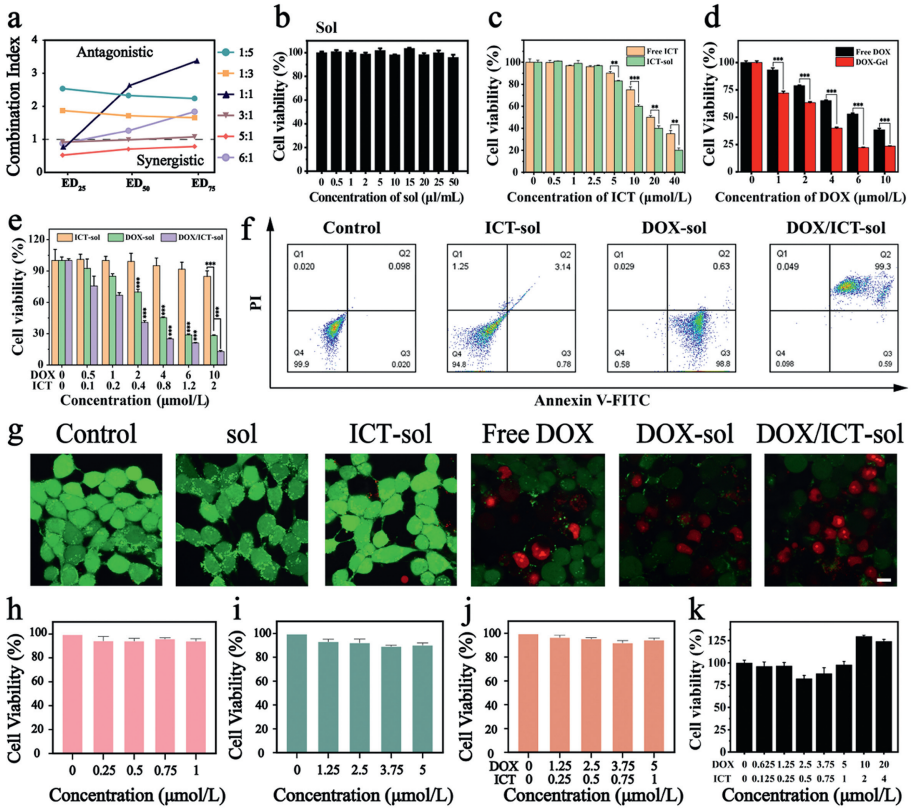


Fig. 2. Cytotoxicity analyses of DOX/ICT-sol on K7M2 cells. (a) CI values for different DOX and ICT ratios. Cytotoxicity analysis of (b) Sol, (c) free ICT *vs.* ICT-sol, (d) free DOX *vs.* DOX-sol, and (e) DOX/ICT-sol on K7M2 cells after 24 h coincubation. (f) Flow cytometry analysis of K7M2 cell necrosis and apoptosis. (g) Live/dead staining of K7M2 cells (green: live cells; red: dead cells). Scale bar: 10 μm. L02 cells viability after 24 h incubating with (h) ICT-sol, (i) DOX-sol and (j) DOX/ICT-sol. (k) MSCs viability after 24 h incubating with DOX/ICT-sol. All data are presented as mean ± SD ($n = 3$). The significant difference is determined by the one-way analysis of variance (ANOVA). $^{**}P < 0.01$, $^{***}P < 0.001$.

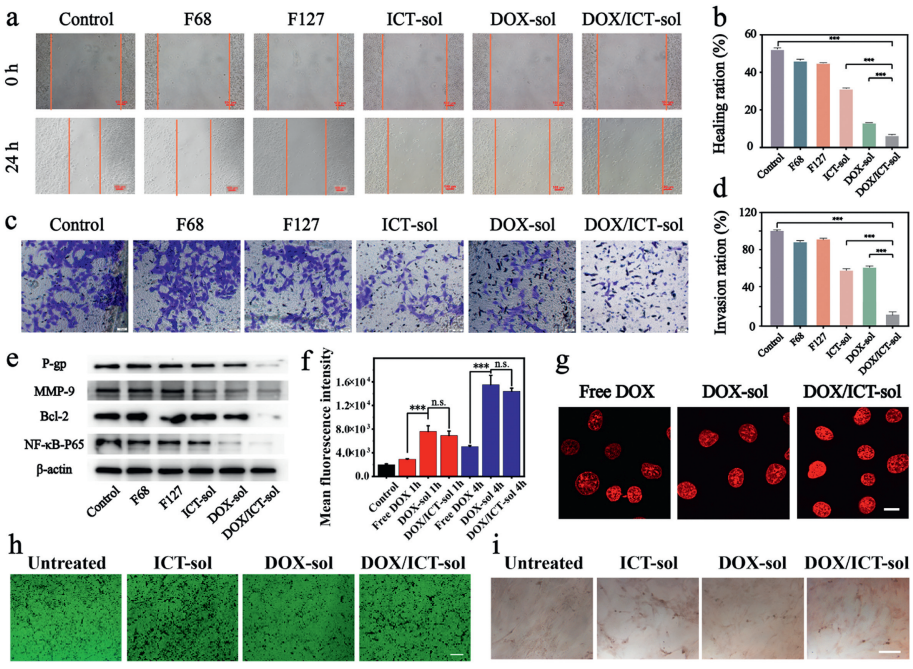


Fig. 3. Inhibitory effect on metastasis and invasion generated by DOX/ICT-sol. (a) Images of K7M2 cells wound at 0 and 24 h after incubation with F68, F127, ICT-sol, DOX-sol and DOX/ICT-sol. Scale bar: 100 μm. (b) The quantification of the healing ratio. (c) Images of the invasive K7M2 cells after cultured for 24 h with F68, F127, ICT-sol, DOX-sol and DOX/ICT-sol on the transwell. Scale bar: 50 μm. (d) The quantification of the invasion ratio. (e) The expression of P-gp, MMP-9, Bcl-2 and NF-κB-P65 in K7M2 cells after receiving different treatments. (f) The mean fluorescence intensity of K7M2 cells after incubation with free DOX, DOX-sol and DOX/ICT-sol at 1 h and 4 h by flow cytometry. (g) The uptake of DOX in K7M2 cells after incubation with different groups. Scale bar: 5 μm. (h) Alkaline phosphatase staining. Scale bar: 100 μm. (i) Alizarin red staining results of stem cells after incubation with different groups. Scale bar: 100 μm. All data are presented as mean ± SD. The significant difference is determined by the one-way ANOVA. ns, no significance. $^{***}P < 0.001$.

proteinase, is involved in the breakdown of the extracellular matrix and is crucial for OS metastasis and invasion [46–48]. Previous studies have identified NF-κB-p65 as a target of ICT, which inhibits its translocation to the nucleus, thus reducing MMP-9 expression and hindering cell invasion. And ICT can also inhibit Bcl-2 expression, contributing to the promotion of apoptosis. Western blot analysis confirmed that treatment with DOX/ICT-sol significantly reduced the expression of NF-κB-p65, Bcl-2, MMP-9, and P-gp in K7M2 cells, indicating that ICT plays a key role in modulating these pathways (Fig. 3e and Fig. S7 in Supporting information). We also examined the intracellular accumulation of DOX in the different treatment groups. As shown in Fig. S8a (Supporting information), the addition of free ICT could significantly increase free DOX uptake ($P < 0.05$). Fig. 3f and Fig. S8b (Supporting information) show that DOX-sol and DOX/ICT-sol both significantly increased DOX cellular accumulation compared to free DOX, with more than a twofold increase in cellular uptake ($P < 0.001$). However, no significant difference in uptake was observed between DOX-sol and DOX/ICT-sol, suggesting that ICT did not play the main role in the enhancement of DOX uptake by the DOX/ICT-sol formulation. This result may be attributed to F127/F68 in the gel formulation, which promoted DOX uptake by enhancing the interaction with the cell membrane and inhibiting P-gp ATPase activity [49–51]. The intracellular location of DOX was also detected with laser scanning confocal microscopy (LSCM). Fig. 3g illustrates that DOX is mainly located in the nucleus. This confirms that the incorporation of F68/F127 and ICT did not alter the subcellular localization of DOX, allowing it to exert its cytotoxic effects effectively.

To further evaluate the osteogenic potential of DOX/ICT-sol, we performed osteogenic differentiation assays using MSCs. Alkaline phosphatase (ALP) staining and Alizarin Red S staining were conducted to assess osteoblast mineralization and extracellular matrix calcification. ALP is a key enzyme marker for mature osteoblasts, and the formation of calcium nodules is a characteristic feature of osteoblast activity [52]. For the ALP staining, MSCs were isolated from rat adipose tissue and seeded in 6-well plates. After 24 h of incubation with ICT-sol, DOX-sol, and DOX/ICT-sol, the cells were fixed and stained using the Gomori calcium-cobalt method. As shown in Fig. 3h, the presence of black staining indicates ALP activity. Significantly higher ALP expression was observed in the ICT-sol and DOX/ICT-sol groups. Next, Alizarin Red staining was used to visualize the formation of calcium nodules. Stem cells were seeded in 6-well plates and incubated with different treatments for 10 days. Alizarin Red is an anthraquinone derivative that binds to calcium ions, producing stable orange-red or deep-red complexes, which allow for the detection of intracellular calcium deposits and mineralized osteoblast nodules. As shown in Fig. 3i, the ICT-sol and DOX/ICT-sol groups exhibited increased intracellular calcium deposits, and small mineralized nodules were observed in these groups, indicating enhanced osteogenic differentiation. These results suggest that the incorporation of ICT not only enhances the anticancer efficacy of DOX but also promotes bone regeneration, highlighting the potential of DOX/ICT-sol for bone-filling therapies in the treatment of OS [53].

We next established an orthotopic OS model in BALB/c mice to further investigate its therapeutic potential. K7M2 cells (2×10^6) were injected into the bone marrow cavity of the tibial bones of mice to generate the OS tumor model [54]. All animal experiments were approved by the Institutional Animal Care and Use Committee of China Pharmaceutical University and conducted in accordance with its ethical guidelines. To evaluate the retention of the hydrogel at the tumor site after intratumoral injection, the fluorescence intensity of DOX emission at 605 nm under blue fluorescence excitation was monitored by fluorescence imaging. DOX-gel and DOX/ICT-gel were locally injected into osteosarcoma, and mice were imaged on days 1, 2, 3, 5, and 7. Major organs were collected

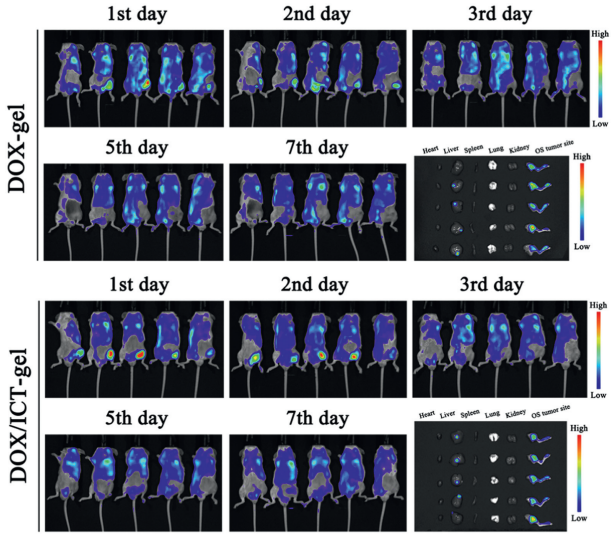


Fig. 4. *In vivo* retention and degradation study of different gel systems. The fluorescence imaging of OS model mice after injection with DOX-gel or DOX/ICT-gel, the fluorescence is the signal of DOX.

and photographed on day 7. Local fluorescence intensity analysis of the administration site and major organs was performed using analysis software after the experiment. As shown in Fig. 4 and Fig. S9a (Supporting information), fluorescence was continuously detected at the injection site until day 7, indicating that local administration of DOX-gel and DOX/ICT-gel can ensure the long-term local retention of DOX. The DOX accumulation in the injection site dissected 7 days after injection was higher than that in the liver (Fig. S9b in Supporting information), indicating that the DOX/ICT-gel formulation can effectively retain the DOX at the tumor site for 7 days, thereby potentially enhancing its therapeutic effect.

The anticancer efficacy of DOX/ICT-gel was evaluated in an orthotopic OS model following the experimental procedure outlined in Fig. 5a. Once the tumor volume reached approximately 80 mm^3, the tumor-bearing mice were randomly assigned to seven treatment groups: PBS, gel (F127/F68), free ICT, ICT-gel, free DOX, DOX-gel, and DOX/ICT-gel (with DOX at 10 mg/kg and ICT at 2 mg/kg). Different formulations were injected into the tumor on days 0 and 8 to ensure consistency in drug distribution and metabolism. Tumor volume and body weight were measured every two days to monitor the anticancer effect and mouse survival status. Mice were sacrificed on day 16 for further histological analysis. As shown in Fig. 5b, the tumors in the PBS, gel, free ICT and ICT-gel groups grew rapidly with little inhibition. In contrast, the free DOX and DOX-gel groups exhibited slower tumor growth, but the most significant inhibition was observed in the DOX/ICT-gel group. The DOX/ICT-gel group showed sustained tumor growth inhibition, with the tumor volume remaining relatively stable over the course of the study. These findings were further corroborated by the tumor weight data (Figs. 5c and d), which showed a significant reduction in the DOX/ICT-gel group compared to other groups. Overall, these results suggest that DOX/ICT-gel provides superior anticancer efficacy compared to single-agent treatments, demonstrating enhanced inhibition of K7M2 tumor growth.

Importantly, a significant decrease in body weight was observed in the free DOX group ($P = 0.01$ compared with the PBS group) throughout the 16-day observation period (Fig. S10 in Supporting information). At the same time, the normal structures of red and white pulp disappeared in the spleen sections of free DOX-treated mice at the end of the experiment (Fig. S11 in Supporting information). These findings indicate that a single local injection of a large

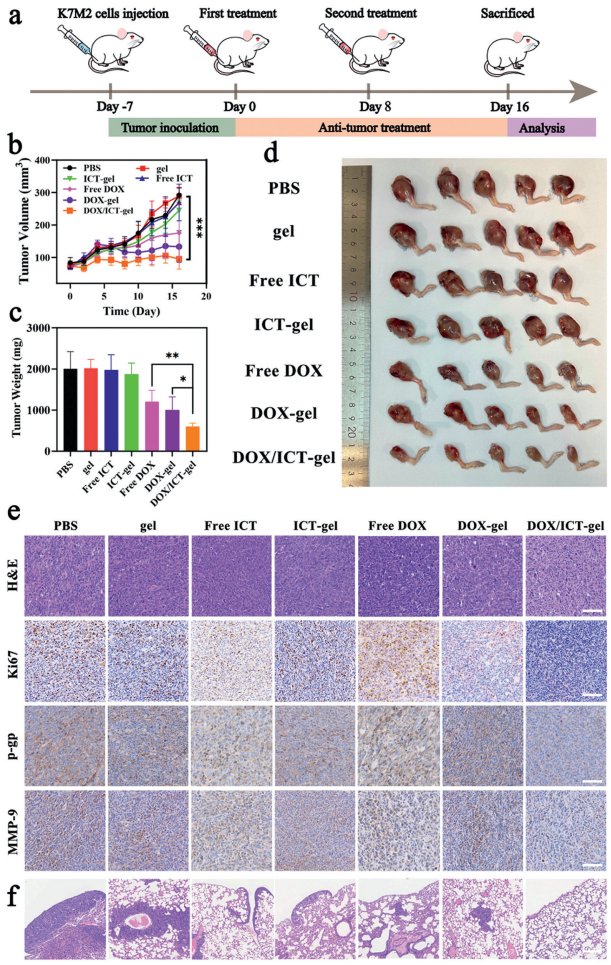


Fig. 5. Anticancer effect of DOX/ICT-gel on OS model mice. (a) Schedule of anticancer treatment regimen. (b) Tumor volumes during anticancer therapy. (c) Tumor weight at the end of the anticancer research. (d) Tumor images of the harvested tumors after anticancer therapy. (e) H&E staining, Ki67, P-gp immunohistochemistry staining, and MMP-9 immunohistochemistry staining of tumor slices collected from different groups (scale bar: 100 μm). (f) The H&E staining of the lungs from different groups (scale bar: 200 μm). Data are presented as mean ± SD ($n = 5$). $^{*}P < 0.05$, $^{**}P < 0.01$, $^{***}P < 0.001$.

dosage of free DOX (10 mg/kg) will cause damage to the body. In contrast, no significant weight loss or damage to important tissues was observed in the other treatment groups, suggesting that the treatments did not cause serious systemic toxicity. Combined with the results that doxorubicin mainly accumulates at the injection site and can release the drug for a long time, these findings indicate that DOX/ICT gel has a good safety profile [55].

Tumor tissues from the different treatment groups were collected and analyzed using hematoxylin and eosin (H&E) staining, and immunohistochemistry was also applied to assess the expression of Ki67, P-gp and MMP-9. As shown in Fig. 5e, cells in the PBS, gel, free ICT, ICT-gel, free DOX and DOX-gel treatment groups exhibited tightly packed, compact morphologies, with indistinct nuclear and cytoplasmic boundaries. In contrast, the cells in the DOX/ICT-gel group showed clearer cytoplasmic boundaries and smaller nuclei, indicating a reduction in tumor malignancy and cellular integrity [56]. Ki67 staining revealed that the free DOX group exhibited significantly higher Ki67 expression, suggesting a potential tumor rebound effect or insufficient suppression of proliferation with DOX alone. Since Ki67 is widely recognized as a marker for cell proliferation and is associated with the aggressiveness of OS [21], the elevated Ki67 levels in the free DOX group suggest that this treatment may inadvertently promote tumor growth and potentially increase the risk of drug resistance and metastasis. In contrast, Ki67 expression was significantly reduced in tumors treated with DOX/ICT-gel, indicating that the combination therapy effectively suppressed tumor cell proliferation. This reduction in Ki67 expression, along with the apoptotic features observed in H&E staining, further supports that DOX/ICT-gel not only inhibits tumor growth but also promotes apoptosis, enhancing its therapeutic efficacy. Additionally, the expression of P-gp and MMP-9 was significantly downregulated in the DOX/ICT-gel group, which is consistent with the mechanism of ICT's action in modulating MDR and tumor invasion. Fig. 5f shows the H&E staining results of lung tissue. The areas with darker purple, enlarged nuclei, and irregularly arranged cells in the sections are the metastatic areas of OS. These results collectively indicate that DOX/ICT-gel enhances the anticancer effects of DOX by downregulating P-gp, mitigating drug resistance, and suppressing local metastasis with the downregulation of MMP-9.

In summary, we have successfully developed an ICT-conjugated, double-sensitizing thermosensitive hydrogel using F68 and F127 as the matrix for effective OS treatment with DOX. The thermosensitive nature of the hydrogel ensures that the DOX/ICT-gel remains localized and evenly distributed at the tumor site, providing sustained and controlled drug release over time. Upon injection, DOX is absorbed by tumor cells and accumulates in the nucleus, where it induces DNA damage. Meanwhile, ICT and Pluronics help to enhance DOX's intracellular concentration. This combination leads to apoptosis of OS cells by downregulating NF-κB and Bcl-2 expression, while simultaneously preventing tumor metastasis by suppressing MMP-9 expression. The DOX/ICT-gel formulation demonstrated significant anticancer efficacy, inhibited metastasis both *in vitro* and *in vivo*, and showed excellent biocompatibility in animal studies. Additionally, ICT's ability to promote osteoblast differentiation suggests the potential for the hydrogel system to be used in postoperative chemotherapy for bone cancer and performs great potential for aiding in bone regeneration after surgical resection. Furthermore, ICT has been shown to remodel the TME, particularly by inducing mitophagy and promoting immunogenic cell death (ICD). The potential for ICT to modulate the TME and influence MSCs, driving their differentiation into osteoblasts, presents a promising avenue for future studies. While our current focus is on the direct cytotoxic and metastasis-inhibiting effects of the DOX/ICT-gel on OS, ICT's potential immune-modulating and bone-regenerating effects, particularly through its impact on MSCs, warrant further investigation. Overall, this thermosensitive hydrogel system provides a promising strategy for more effective osteosarcoma treatment, reducing the toxic side effects of DOX while enhancing therapeutic efficacy. The combination of ICT and DOX offers a potent, low-toxicity, high-efficiency treatment option, providing important insights for the development of alternative therapies for OS.

Declaration of competing interest

The authors declare that they have no known competing financial interests or personal relationships that could have appeared to influence the work reported in this paper.

CRediT authorship contribution statement

Qing-Ri Jin: Writing – original draft, Conceptualization. **Tian-Jiao Zhou:** Writing – original draft, Formal analysis, Data curation. **Ya-Ting Yao:** Project administration, Methodology, Investigation. **Hai-Qing Yu:** Methodology, Investigation. **Hao-Bin Che:** Methodology. **Meng-Meng Zhang:** Methodology. **Chun-Hui Cui:**

Investigation. **Yi Wang:** Funding acquisition. **Cheng-Jun Li:** Writing – review & editing, Funding acquisition. **Lei Xing:** Writing – review & editing, Funding acquisition. **Hu-Lin Jiang:** Writing – review & editing, Supervision.

Acknowledgments

This work was financially supported by the National Key R&D Program of China (No. 2022YFE0198400), National Natural Science Foundation of China (Nos. 82020108029, 82073398, 82473867 and 82302367), Natural Science Foundation of Jiangsu Province (No. BK20231019), Project of State Key Laboratory of Natural Medicines, China Pharmaceutical University (No. SKLNMZZ202021), Double First-class University Projects (No. CPU2018GY06), Double First-Rate construction plan of China Pharmaceutical University (No. CPU2022QZ18).

Supplementary materials

Supplementary material associated with this article can be found, in the online version, at doi:10.1016/j.cclet.2025.111539.

References

[1] J. Ritter, S.S. Bielack, Ann. Oncol. 21 (2010) vii320–vii325.
[2] L.C. Sayles, M.R. Breese, A.L. Koehne, et al., Cancer Discov. 9 (2019) 46–63.
[3] H.C. Beird, S.S. Bielack, A.M. Flanagan, et al., Nat. Rev. Dis. Primers. 8 (2022) 77.
[4] R.L. Siegel, K.D. Miller, A. Jemal, CA Cancer J. Clin. 70 (2020) 7–30.
[5] C.K. Lettieri, N. Appel, N. Labban, et al., Immunotherapy 8 (2016) 1233–1244.
[6] R. Rathore, B.A. Van Tine, J. Clin. Med. 10 (2021) 1182.
[7] J. Gill, R. Gorlick, Nat. Rev. Clin. Oncol. 18 (2021) 609–624.
[8] M. Gu, W. Yu, S.T. Stefanello, et al., J. Control. Release 377 (2025) 174–185.
[9] K. Igarashi, K. Kawaguchi, S. Li, et al., Cancer Lett. 417 (2018) 168–173.
[10] C.M. Hattinger, M. Fanelli, E. Tavanti, et al., Expert Opin. Emerg. Drugs 20 (2015) 495–514.
[11] S.E. Lipshultz, R. Karnik, P. Sambatakos, et al., Curr. Opin. Cardiol. 29 (2014) 103–112.
[12] Y. Cao, X. Ge, Y. Wei, et al., Chin. Chem. Lett. 35 (2024) 108672.
[13] S. Zhang, X. Liu, T. Bawa-Khalfe, et al., Nat. Med. 18 (2012) 1639–1642.
[14] S.S. Bielack, B. Kempf-Bielack, G. Delling, et al., J. Clin. Oncol. 20 (2002) 776–790.
[15] L. Kager, A. Zoubek, U. Pötschger, et al., J. Clin. Oncol. 21 (2003) 2011–2018.
[16] S. Wang, K. Yu, Z. Yu, et al., Chin. Chem. Lett. 34 (2023) 108184.
[17] F. Shen, W.S. Cai, J.L. Li, et al., Onco Targets. Ther. 7 (2014) 305–314.
[18] J. Chen, W. Wang, H. Wang, et al., Drug Discov. Ther. 8 (2014) 33–41.
[19] C. Zhang, J. Niu, J. Li, et al., Chin. Chem. Lett. 35 (2024) 108556.
[20] J. Li, S. Shen, Z. Liu, et al., J. Nat. Prod. 86 (2023) 290–306.
[21] M. Seiti, P.S. Ginestra, R.M. Ferraro, et al., Int. J. Bioprint. 8 (2022) 504.
[22] Z. Yu, J. Guo, M. Hu, et al., ACS Nano 14 (2020) 4816–4828.
[23] L. Huang, X. Wang, H. Cao, et al., Biomaterials 182 (2018) 58–71.
[24] Q. Wang, Q. Liang, J. Dou, et al., Nat. Nano 19 (2024) 95–105.
[25] Z. Li, W. Xu, J. Yang, et al., Adv. Mater. 34 (2022) e2200449.
[26] T.J. Zhou, L. Xing, Y.T. Fan, et al., J. Control. Release 307 (2019) 44–54.
[27] Y. Feng, Z. Zhang, W. Tang, Y. Dai, Exploration 3 (2023) 20220173.
[28] R. Tian, X. Qiu, W. Mu, et al., Chin. Chem. Lett. 35 (2024) 108343.
[29] Y. Feng, Z. Zhang, W. Tang, et al., Exploration 3 (2023) 20220173.
[30] J. Li, D.J. Mooney, Nat. Rev. Mater. 1 (2016) 16071.
[31] Q. Luo, J. Sun, Z. Li, et al., Chin. Chem. Lett. 36 (2025) 110433.
[32] N.U. Khaliq, J. Lee, S. Kim, et al., Pharmaceutics 15 (2023) 2102.
[33] T.J. Zhou, L. Xing, Y.T. Fan, et al., J. Control. Release 309 (2019) 82–93.
[34] L.S. Yap, M.C. Yang, Colloids Surf. B 185 (2020) 110606.
[35] M.M. Al-Rajabi, Y.H. Teow, Sustain. Chem. Pharm. 31 (2023) 100939.
[36] A.V. Kabanov, E.V. Batrakova, V.Y. Alakhov, Adv. Drug Deliv. Rev. 54 (2002) 759–779.
[37] C. Pérez-Arnaiz, N. Busto, J.M. Leal, et al., J. Phys. Chem. B 118 (2014) 1288–1295.
[38] M. Lashkari, A. Fatemi, H.M. Valandani, et al., Sci. Rep. 12 (2022) 12657.
[39] T.J. Zhou, M.M. Zhang, D.M. Liu, et al., Biomaterials 305 (2024) 122447.
[40] Y. Jin, G. Han, Y. Gao, et al., Nat. Commun. 16 (2025) 2022.
[41] L. Zhang, Y.X. Liu, Y.T. Yao, et al., Int. J. Pharm. 634 (2023) 122637.
[42] D.D. Ilchovska, D.M. Barrow, Autoimmun. Rev. 20 (2021) 102741.
[43] X. Wu, Z. Cai, L. Lou, Y. Zhu, Cancer Epidemiol. 36 (2012) 212–216.
[44] T. Nedelcu, B. Kubista, A. Koller, et al., J. Cancer Res. Clin. 134 (2008) 237–244.
[45] C.J. Ho, H.J. Ko, T.S. Liao, et al., Cell Death. Discov. 7 (2021) 275.
[46] C.J. Lee, T.Y. Jang, S.E. Jeon, et al., Nat. Commun. 15 (2024) 10422.
[47] J. Wang, Q. Shi, T. Yuan, et al., Clin. Chim. Acta 433 (2014) 225–231.
[48] H. Li, K. Zhang, L. Liu, et al., Tumor Biol. 35 (2014) 5487–5491.
[49] E.V. Batrakova, S. Li, A.M. Brynskikh, A.K. Sharma, et al., J. Control. Release 143 (2010) 290–301.
[50] T. Minko, E.V. Batrakova, S. Li, et al., J. Control. Release 105 (2005) 269–278.
[51] V. Alakhov, E. Klinski, S. Li, et al., Colloids Surf. B 16 (1999) 113–134.
[52] Z. Lin, Z. Chen, Y. Chen, et al., Exploration 3 (2023) 20220149.
[53] Y. Luo, Y. Gao, Nano Biomed. Eng. 16 (2024) 188–202.
[54] J. Chang, F. Zhao, X. Sun, et al., J. Vis. Exp. (2021) e63072.
[55] T.J. Zhou, Y. Xu, L. Xing, et al., Adv. Mater. 33 (2021) e2100114.
[56] T.J. Zhou, X. Wan, M.M. Zhang, Biomaterials 300 (2023) 122205.